Results from muon reconstruction performance with ATLAS at Run 3

INFN

ATLAS EXPERIMENT

Marco Sessa
INFN Roma Tor Vergata

May 17th, 2023

34th Rencontres de Blois on "Particle Physics and Cosmology"

Outline

- The ATLAS Muon Spectrometer
  - New Small Wheel Phase 1 upgrade
- Reconstruction algorithms
- Reconstruction and identification efficiency
- Isolation requirements
- Momentum scale and resolution

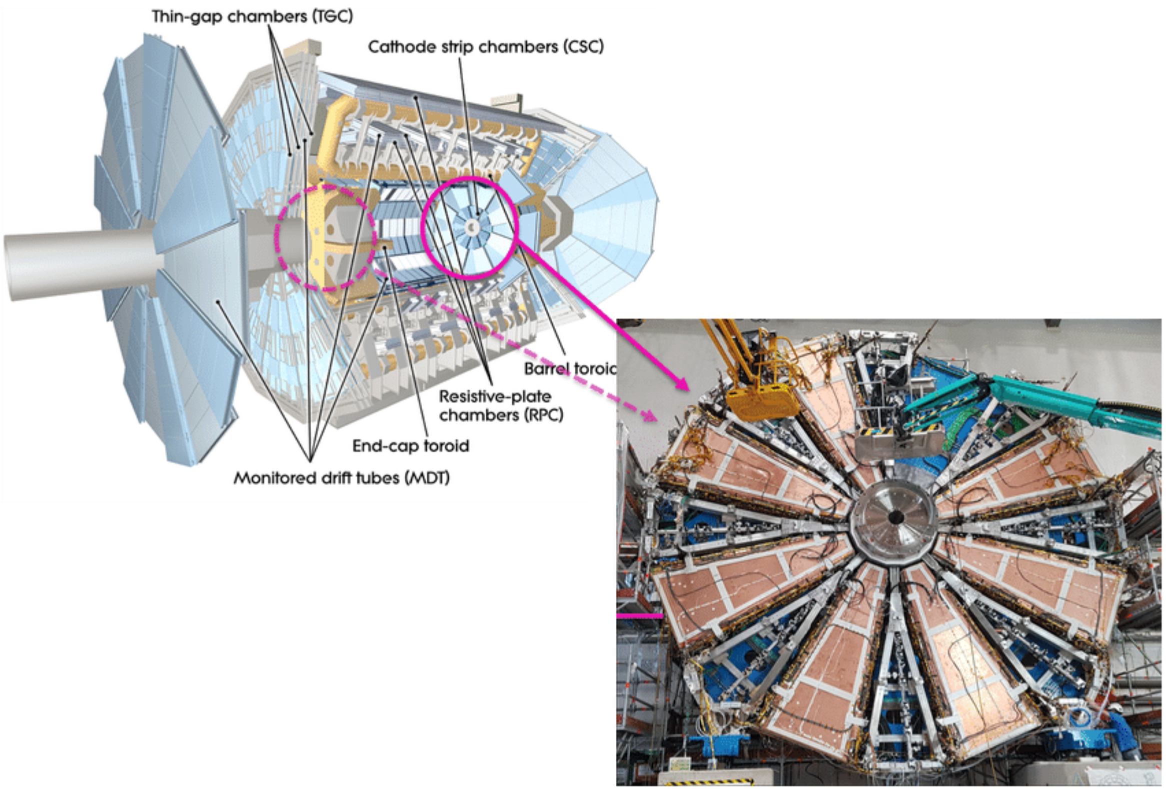

The ATLAS data-taking in 2022

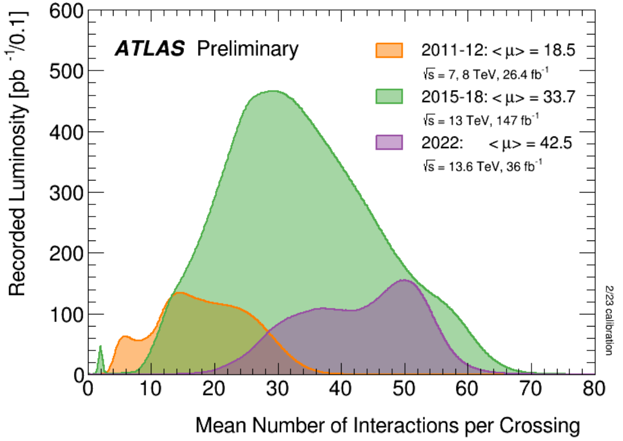

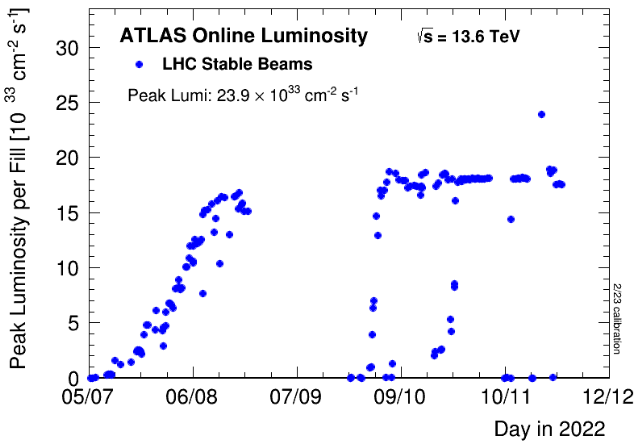

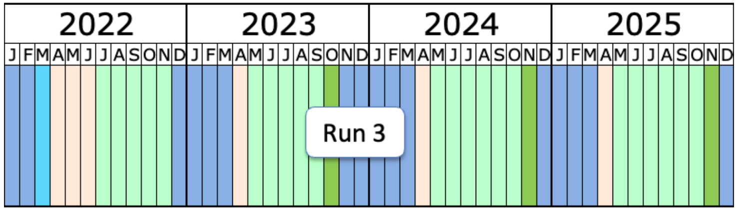

Expected delivered luminosity ~300 fb^{-1}

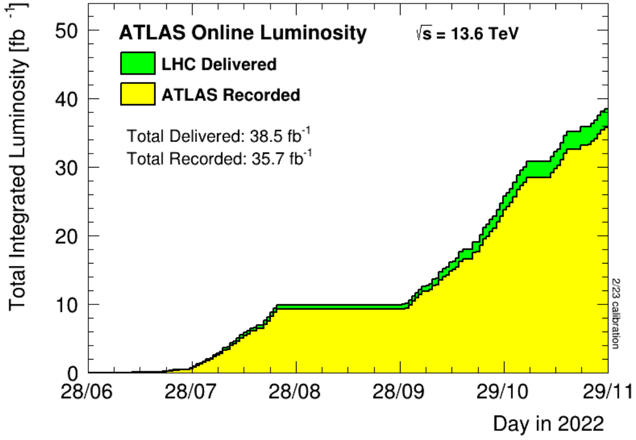

- Run 3 started in 2022
- Average number of pp interactions per bunch crossing ~42.5
- Peak luminosity 2.4 x 10^{34} cm^{-2} s^{-1}
- Recorded integrated luminosity 35.7 fb^{-1}
- 93% recording efficiency

- 2023 data taking just started, first stable beams at 13.6 TeV in mid of April

The ATLAS Muon Spectrometer (MS)

- Designed to identify muon candidates and to measure the muon momentum and charge independently from the Inner Tracker
- Divided in a central region (barrel, |η| < 1.05) and two end-cap regions (1.05 < |η| < 2.7)
- Three toroidal air-core magnets deflect muon tracks in the (r,z) plane, allowing to measure the muon momentum
- Employed detector technologies for the legacy system described below

Trigger detectors

- **Resistive Plate Chambers**
  - Three doublet layers
  - |η| < 1.05
  - Time resolution ~1 ns
- **Thin Gap Chambers**
  - One triplet and two doublet layers
  - 1.0 < |η| < 2.4
  - Timing perf: >99% triggers on the correct BC

Precision tracking detectors

- **Monitored Drift Tubes**
  - Three layers in barrel and two in the end-caps
  - 6-8 η measurements per chamber
  - |η| < 2.7
  - Single hit position resolution ~90 μm

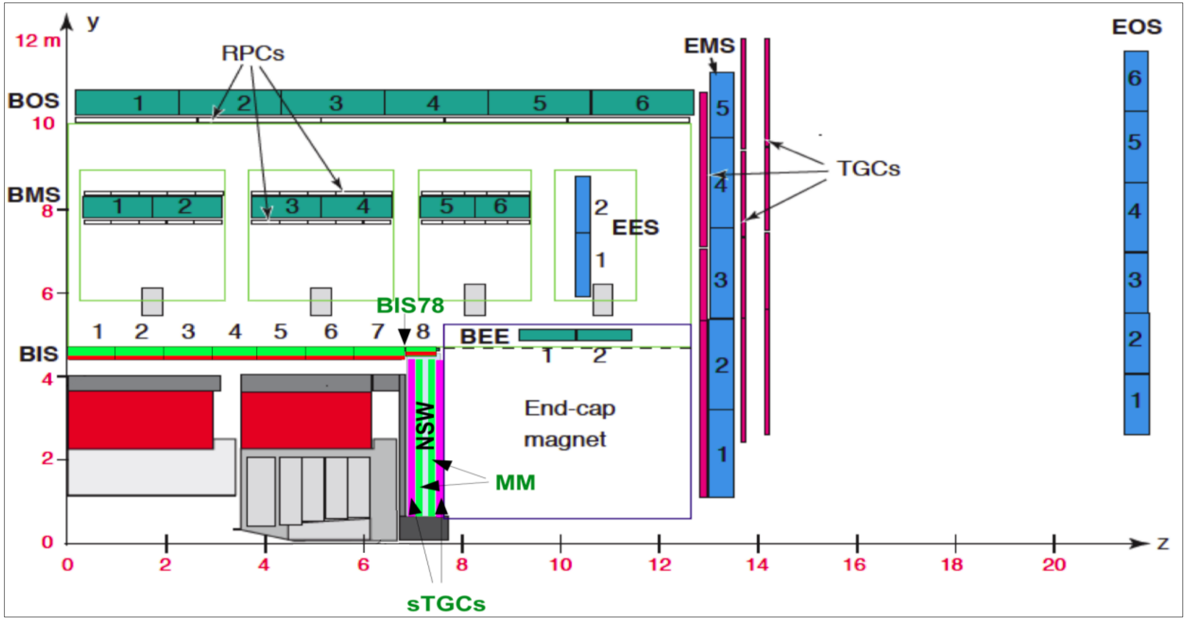

New Small Wheel Phase 1 upgrade

- New Small Wheel Phase 1 upgrade: needed to handle the higher instantaneous luminosity and to reduce the fake trigger rate
- Employed detector technologies: **Micromegas** and **small-strip Thin Gap Chambers**
  - Micromegas → Largest-area MPGD detector employed in HEP experiments so far
- NSW in commissioning during 2022, always included in the ATLAS DAQ

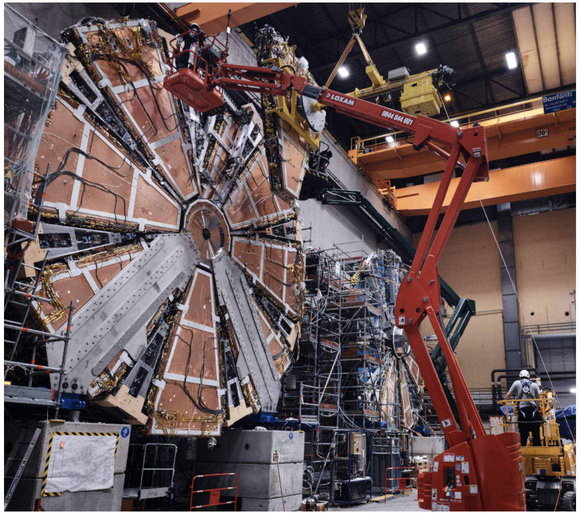

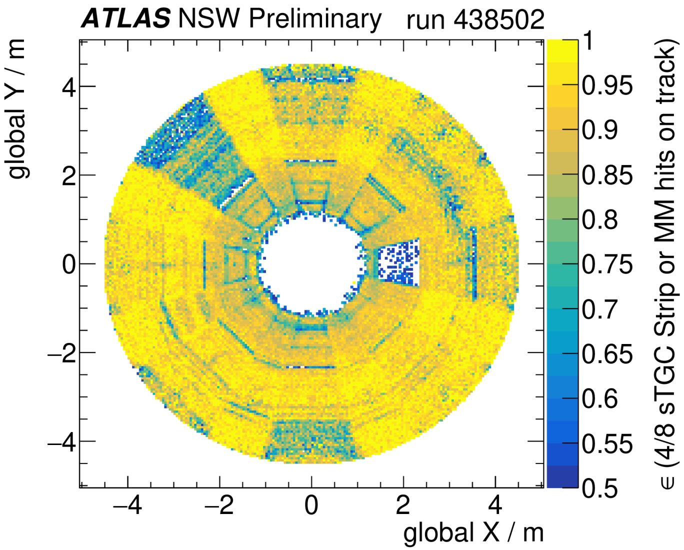

Efficiency affected mainly by DAQ issues during 2022 runs - solved during winter shutdown

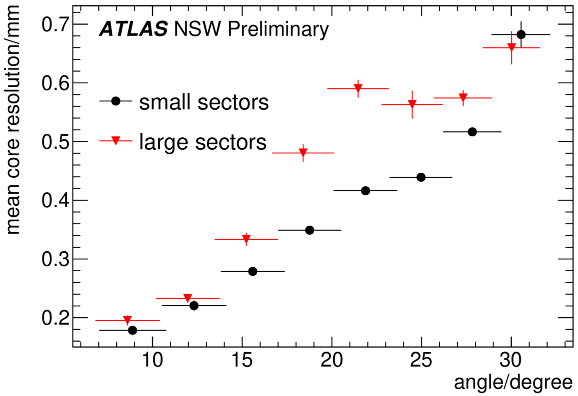

Top: Micromegas position resolution (charge centroid, difference between neighboring layers)

Left: efficiency for having at least four out of eight layers of either Micromegas or sTGC strip associated to a muon track → efficiency with which the NSW is contributing to the reconstruction of the muon track

Muon reconstruction in ATLAS

Eur. Phys. J. C 81 (2021) 578

- The muon reconstruction proceeds according to five main reconstruction algorithms (as shown in the picture)
- **Combined Muons** are identified by matching MS tracks to Inner Tracker tracks and performing a combined track fit based on the MS and Inner Tracker hits, taking into account the energy loss in the calorimeters and multiple scattering
  - More than 95% of muons are Combined Muons and they are generally used for most of the ATLAS physics analyses
- Other reconstruction algorithms help to recover muon reconstruction efficiency for low p_T muons or in regions of limited detector coverage or when parts of the MS or Inner Tracker are inefficient

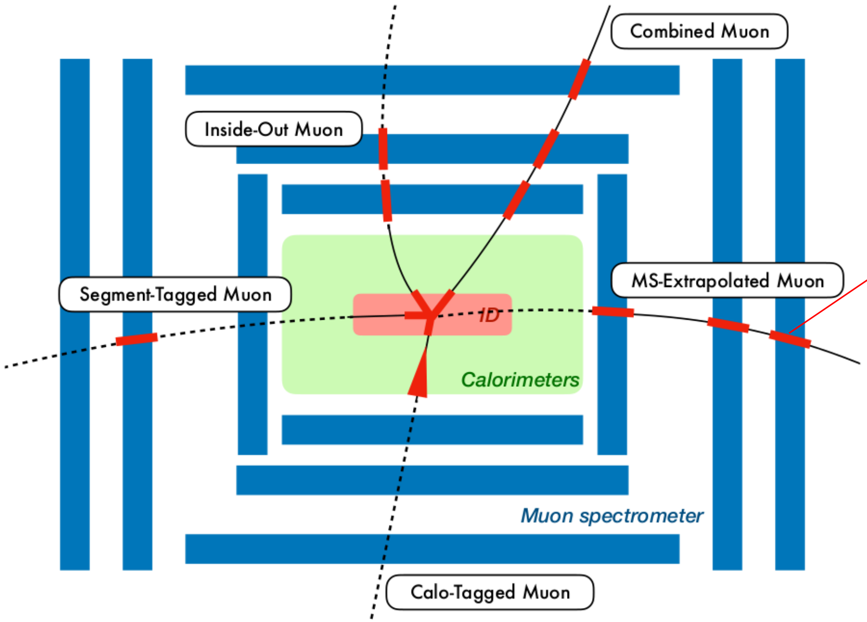

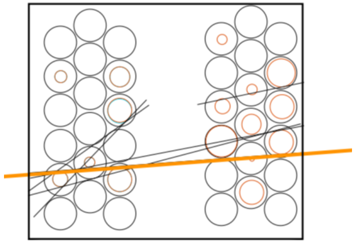

Track segments

MS track reconstruction

1) Track segments are reconstructed in each layer of the MS
- Including trigger hits from RPCs or TGCs to evaluate the ϕ coordinate

2) MS tracks are reconstructed from the segments
- Minimum of two segments required
- Additional hits can be added during the fit
- Including a beam-spot constraint and energy loss

Muon quality working points

Eur. Phys. J. C 81 (2021) 578

- Three standard selection WPs are designed to cover the needs of the ATLAS physics analyses
  - The **Medium** WP provides an efficiency and purity suitable for a wide range of analyses → low systematic uncertainties in the prompt-muon efficiency and background rejection small
  - The **Loose** selection WP optimized for analyses with high muon multiplicity → higher efficiency at the cost of less purity and larger systematic uncertainties
  - The **Tight** selection WP → highest purity → ad hoc for analyses limited by background from non-prompt muons

- Two additional selection WPs are designed for analyses targeting extreme phase space regions: **Low-p_T** and **High-p_T**

From ATLAS Run 2

	$20 < p_T$ [GeV] < 100	
Selection WP	ϵ_μ [%]	ϵ_{had} [%]
Loose	99	0.25
Medium	97	0.17
Tight	93	0.12
Low-p_T (cut-based)	97	0.17
Low-p_T (multivariate)	97	0.17
High-p_T	80	0.13

Fraction of hadrons misidentified as muons

In Run 3, a modified version of the quality WPs with tighter requirements in the NSW region is used, due to the detector commissioning

Muon reconstruction efficiency

MUON-2023-01

- Comparison between Run 2 (left) and Run 3 (right) efficiencies for Medium muons with $p_T > 10$ GeV
- Efficiencies measured using $Z \to \mu\mu$ events with tag-and-probe method
- Efficiency Scale Factors ($\varepsilon_{Data}/\varepsilon_{MC}$) are used to quantify the deviation of the simulation from the real detector behavior and are used in physics analyses to correct the simulation

$Z \rightarrow \mu\mu$

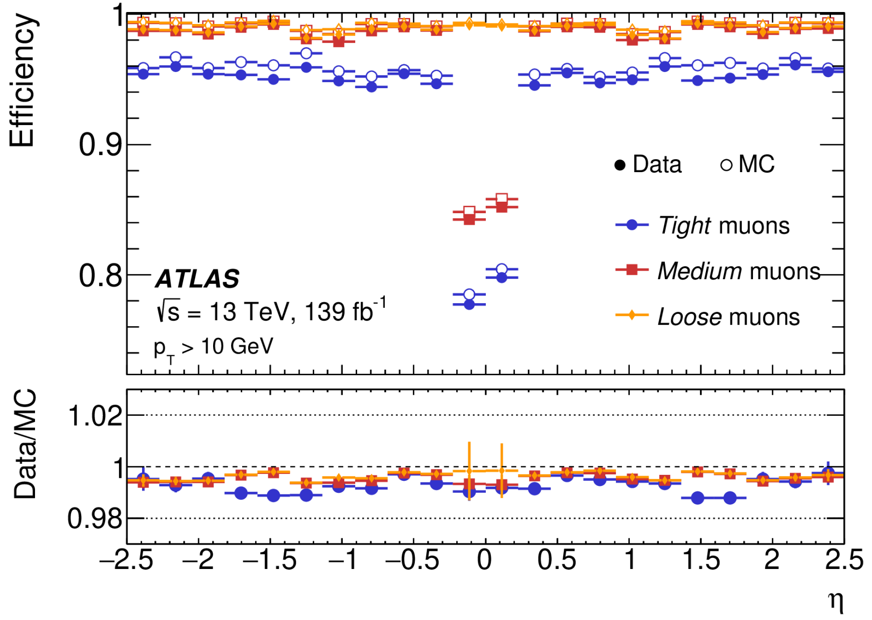

Eff vs phi in different eta regions

Acceptance hole at η~0 due to space for services

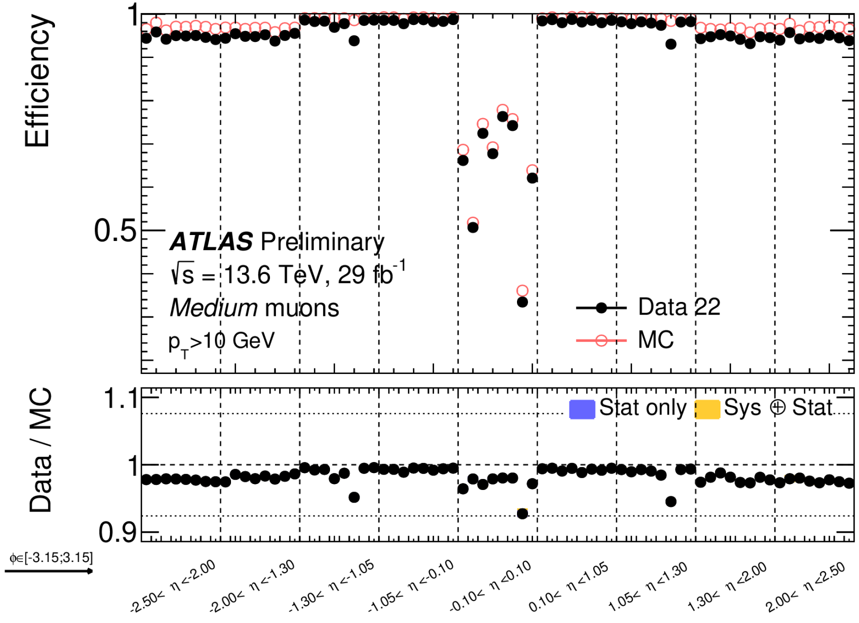

- Very high efficiency in most of the phase space, well described by MC simulation → up to 0.1% precision

Muon isolation efficiency

- Muons from prompt decays of Standard Model bosons can be discriminated from muons from hadronic sources by measuring the amount of hadronic activity in their vicinity
  - Non-promt muons originate from heavy hadrons, taus or heavy quark decays
- Scalar sum of p_T (or E_T) within a cone around the muon track is often used
  - particle-flow algorithms used for some isolation WPs
- Isolation efficiency for muons satisfying a track-based isolation variable (**Tight WP**) is shown a function of the muon p_T

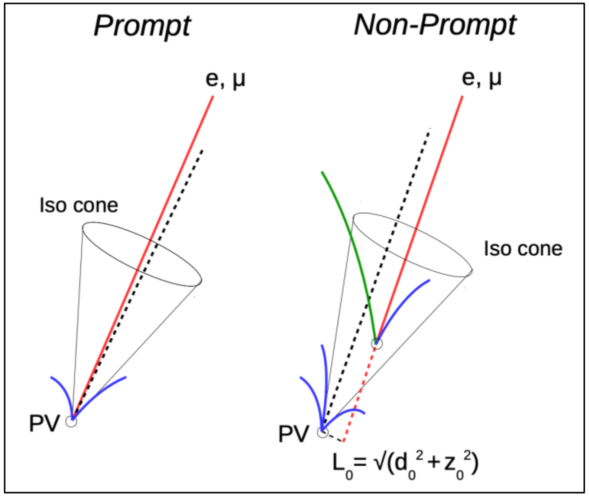

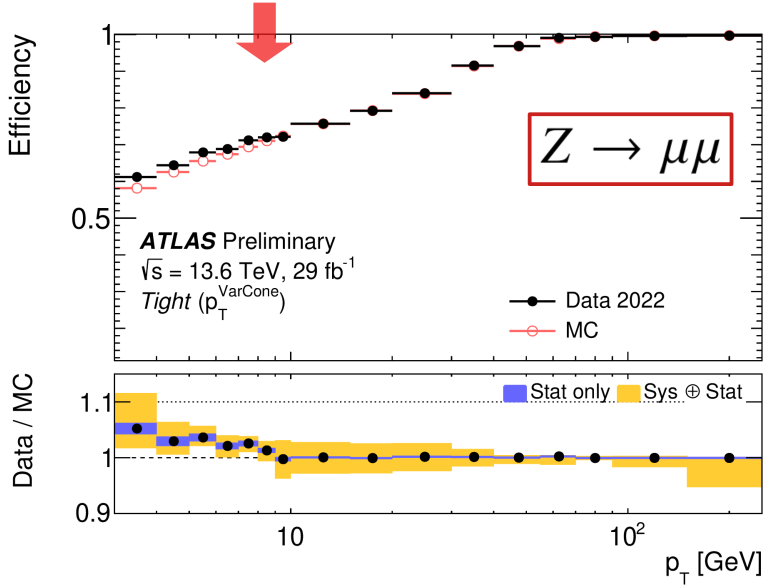

Charge-dependent momentum scale calibration in data

- Residual misalignment, not fully corrected by the standard detector alignment procedures, can induce charge-dependent bias on the muon momentum measurement. It can arise from:
  - geometrical distortions or deformations in the Inner Tracker may not be corrected by global minimization of χ^2 residuals
  - residual uncertainty in the muon alignment system (performed via optical alignment sensors and straight muon tracks → tens of μm precision on the muon sagitta)
- Appropriate set of corrections applied to data (while simulated samples assume ideal detector alignment)
- To estimate and correct the sagitta bias, a large sample of Z→ μμ events is used
- Correction is obtained by an iterative fit, minimizing the variance of Z boson $m_{\mu\mu}$ invariant mass, measured in bins of η and φ

biased

corrected

$$p_T = \frac{\hat{p}_T}{1 - q\,\hat{\delta}_s(\eta,\phi)\,\hat{p}_T}$$

Sagitta bias reduced on average from 0.4 TeV^{-1} up to $2\cdot10^{-4}$ TeV^{-1}

Residual bias on data after applying sagitta bias correction

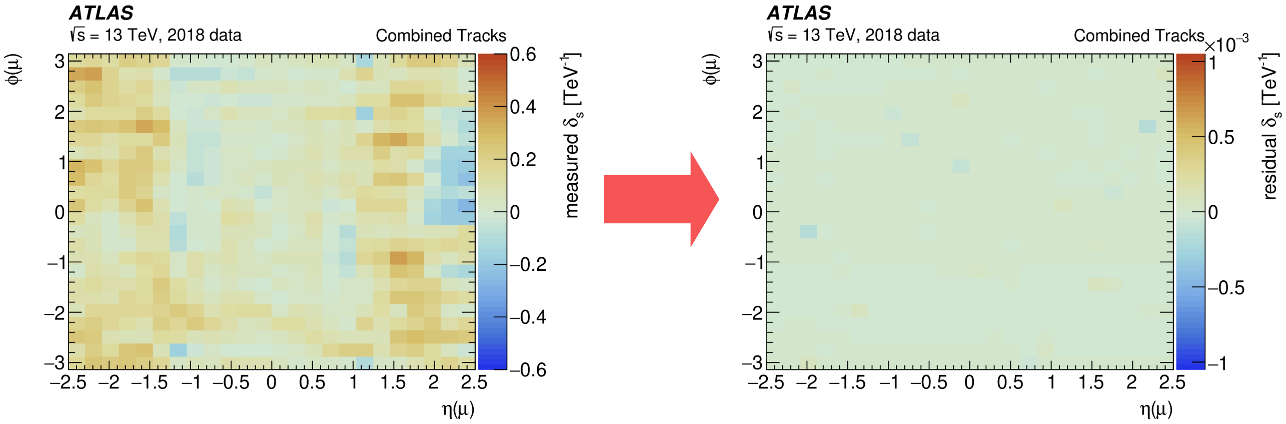

arXiv:2212.07338

Muon momentum calibration procedure in simulation

- Performed to correct the simulation (separately for ID and MS tracks), improving the agreement between data and simulation and reducing the systematic uncertainties related to the muon calibration in physics analyses

- **muon momentum scale correction**
  - s0: inaccuracy in the description of the magnetic field
  - s1: inaccuracy in the simulation of the energy loss in calorimeter

- **muon momentum resolution smearing**
  - Δr0: energy loss fluctuations in the material
  - Δr1: multiple scattering, local distortions of the magnetic field
  - Δr2: intrinsic detector resolution and residual misalignment

$$p_{\mathrm{T}}^{\mathrm{Cor,Det}} = \frac{p_{\mathrm{T}}^{\mathrm{MC,Det}} + \sum_{n=0}^{1} s_n^{\mathrm{Det}}(\eta,\phi)\left(p_{\mathrm{T}}^{\mathrm{MC,Det}}\right)^n}{1 + \sum_{m=0}^{2} \Delta r_m^{\mathrm{Det}}(\eta,\phi)\left(p_{\mathrm{T}}^{\mathrm{MC,Det}}\right)^{m-1} g_m}$$

arXiv:2212.07338

- s and Δr are extracted by fitting the Z and J/Psi invariant mass spectrum and searching for the configuration that provides the best agreement between simulation and data

- Analysis performed in η-ϕ detector regions, homogeneous in detector technology and performance

- Invariant mass distributions for J/Psi → μμ and Z→ μμ candidates compared with the corrected MC simulation

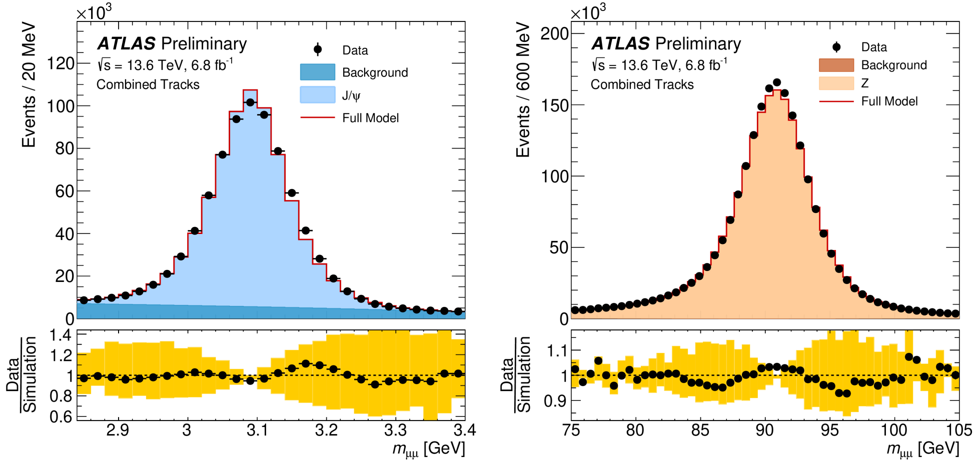

Muon momentum scale

$J/\psi \rightarrow \mu\mu$

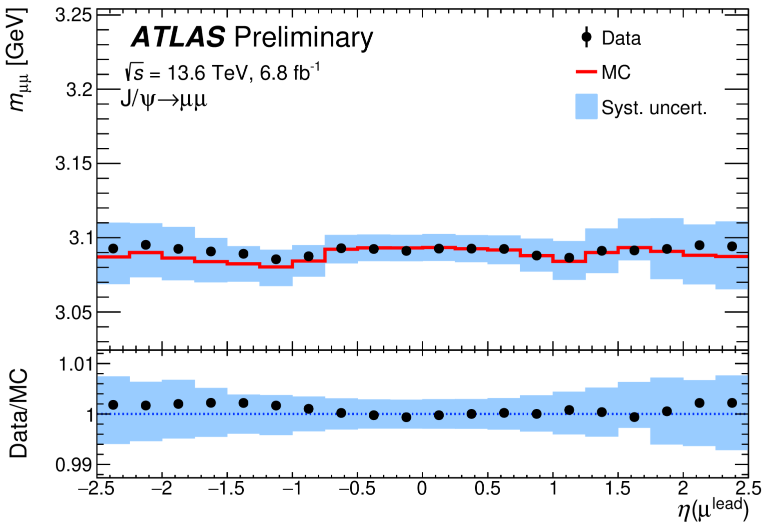

$Z \rightarrow \mu\mu$

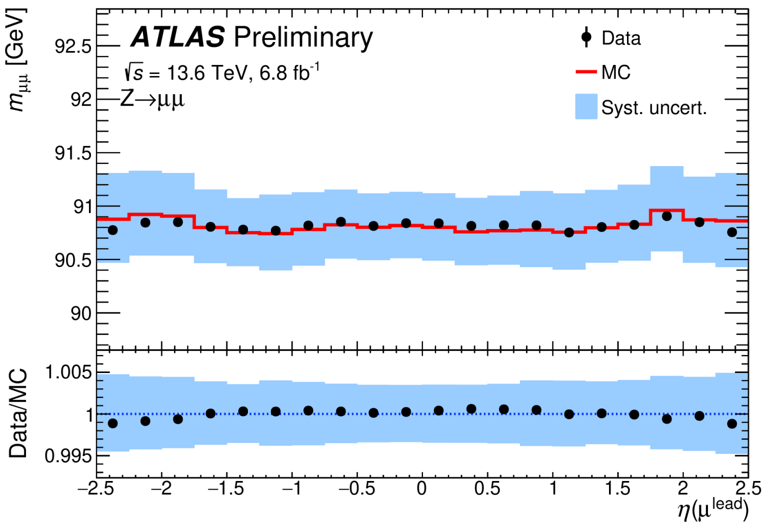

- Sagitta bias correction is not applied to data, not enough statistics to derive it yet
- Data-MC agreement within the uncertainties → few per mille level precision
- Results still based on partial dataset, but calibrations already provided to physics groups with the full 2022 dataset

Muon momentum resolution

MUON-2022-02

$J/\psi \rightarrow \mu\mu$

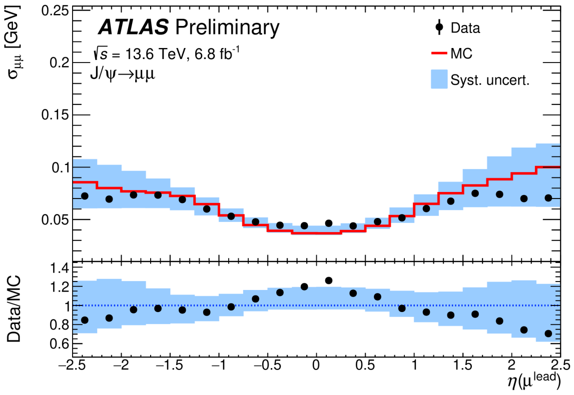

$Z \rightarrow \mu\mu$

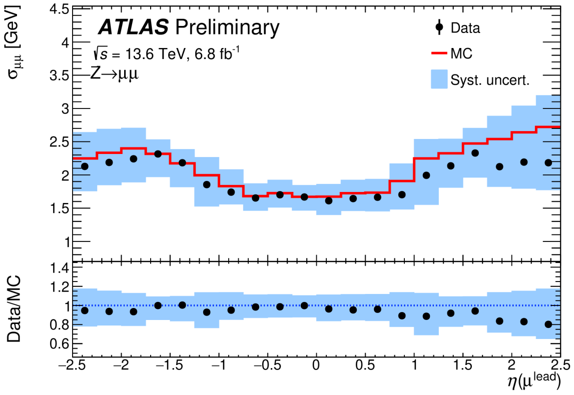

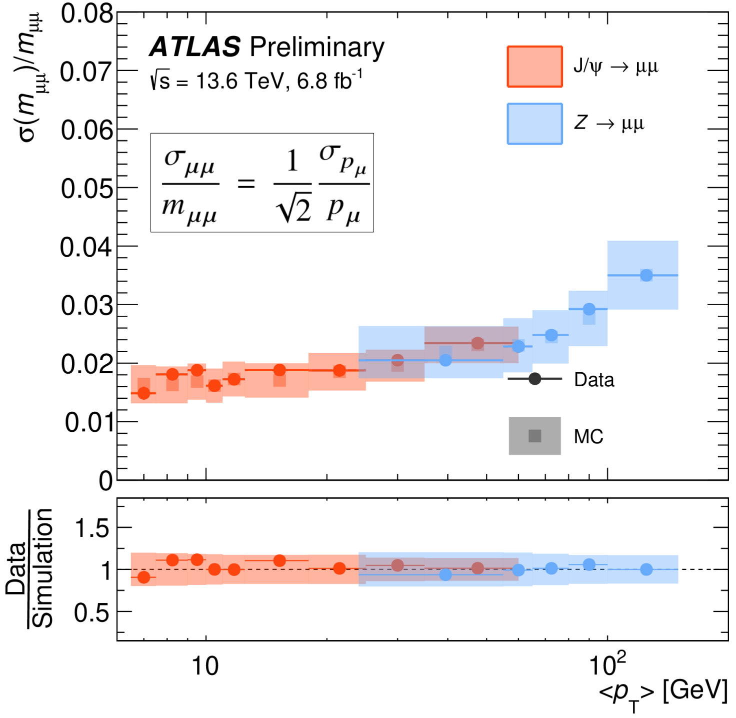

- Data-MC agreement within the uncertainties
- Good agreement in the overlap region between J/Psi and Z measurements
- Large uncertainty due to the low statistics
- Results still based on partial dataset, but calibrations already provided to physics groups with the full 2022 dataset

Muon momentum scale and resolution: Run 2 results

arXiv:2212.07338

$Z \rightarrow \mu\mu$

Working hard to reach this level of precision on Run 3

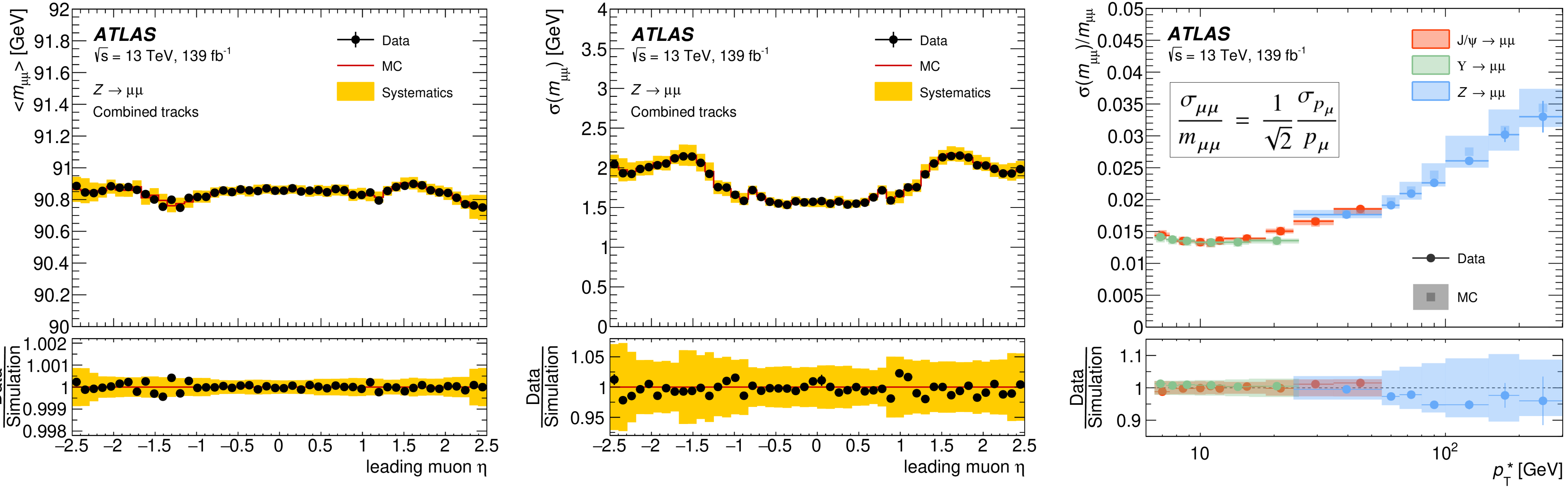

Uncertainty on the momentum scale from a minimum of 0.05% for |η| < 1 to a maximum of 0.15% for |η| ~ 2.5

Di-muon mass resolution from a minimum of 1.6 GeV for |η| < 1 to a maximum of 2.4 GeV for |η| ~ 2.5

Relative di-muon mass resolution from ~1.5% up to ~3.5% in the considered p_T range

Conclusions

28-05-2022, first reconstructed muon with NSW detector

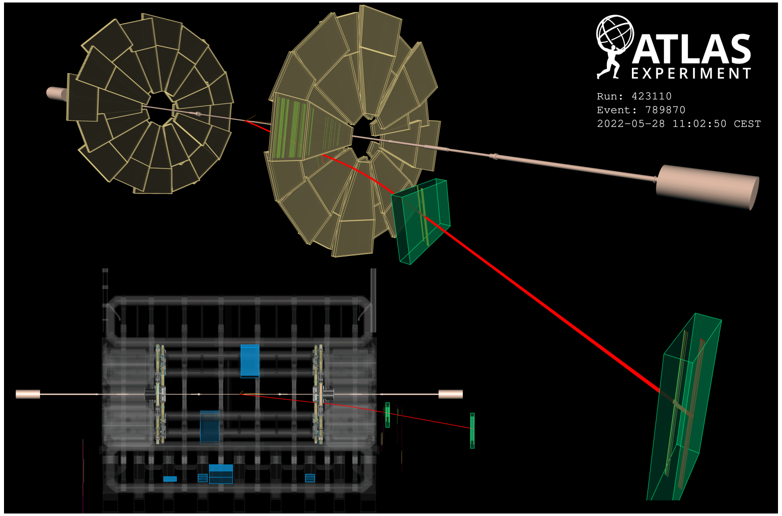

- Presented the strategy and results of muon performance in Run 3
- ATLAS muon reconstruction is working well in Run 3
  - Expect to reach Run 2 levels of performance with sufficient events
- Despite the commissioning of new detectors, momentum and efficiency calibrations already provided and included in the results of the first Run 3 physics analyses (top and Z cross-section measurements) shown at Moriond EW conference

Back-up slides

ATLAS MDT performance

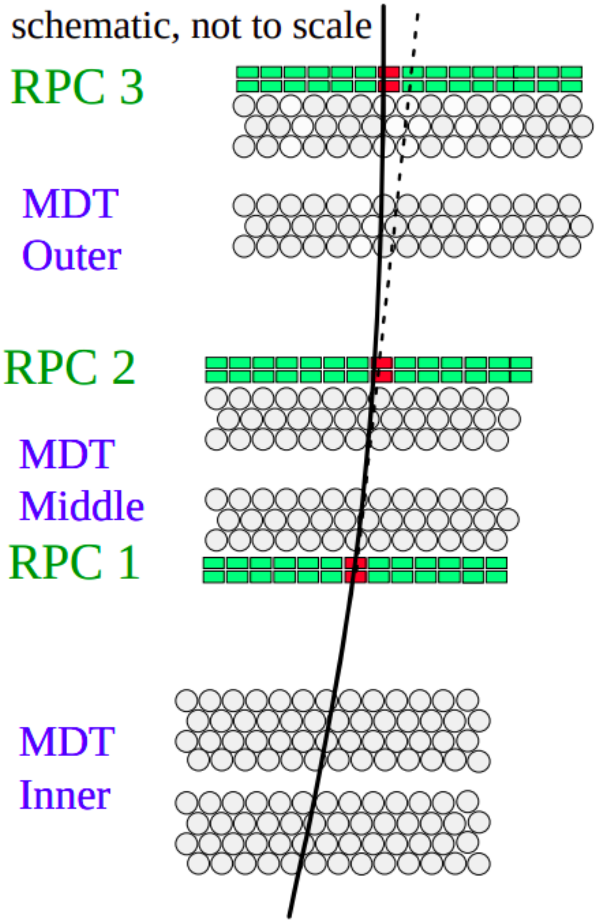

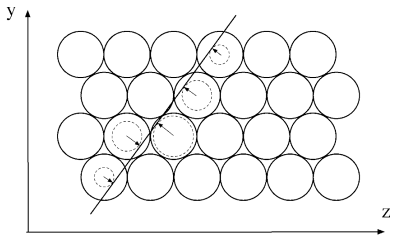

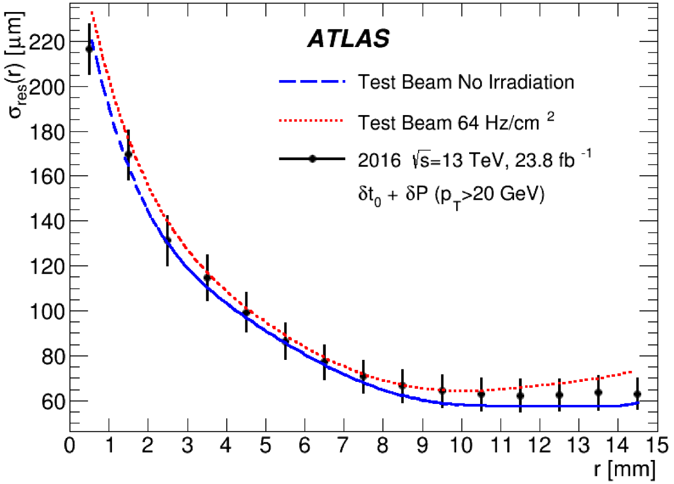

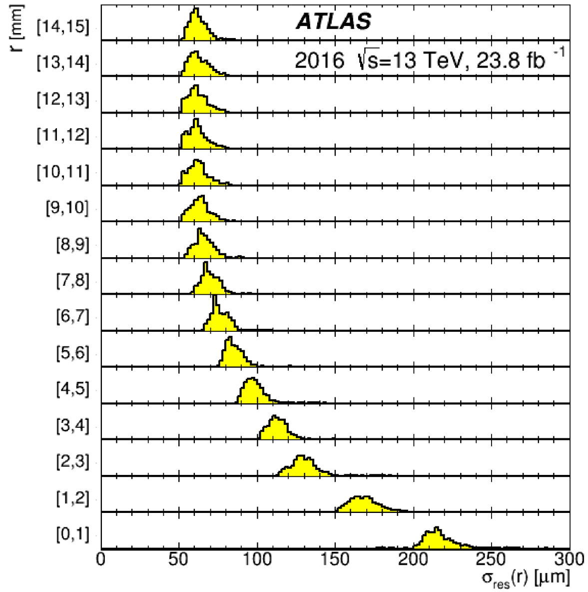

Tube diameter 30 mm

Ar:CO_2 93:7 gas mixture at an absolute pressure of 3 bar

MDT chamber consists of 2 multi-layers with 3 or 4 layers of tubes each

Muon working points in ATLAS Run 2

Table 1: Prompt-muon efficiencies ϵ_{μ} and light-hadron misidentification rates ϵ_{had} for the different selection working points, evaluated in a $t\bar{t}$ MC sample in different p_{T} regions for $|\eta| < 2.5$. It should be noted that the *Tight* WP by construction does not select any muons with $p_{\mathrm{T}} < 4$ GeV, which is reflected in the corresponding efficiency in the first p_{T} region. The statistical uncertainties are at least one order of magnitude smaller than the last digit reported.

	$3 < p_{\mathrm{T}}$ [GeV] < 5		$5 < p_{\mathrm{T}}$ [GeV] < 20		$20 < p_{\mathrm{T}}$ [GeV] < 100		$p_{\mathrm{T}} > 100$ GeV	
Selection WP	ϵ_{μ} [%]	ϵ_{had} [%]	ϵ_{μ} [%]	ϵ_{had} [%]	ϵ_{μ} [%]	ϵ_{had} [%]	ϵ_{μ} [%]	ϵ_{had} [%]
Loose	90	1.17	98	1.06	99	0.25	98	0.12
Medium	70	0.63	97	0.85	97	0.17	97	0.07
Tight	36	0.15	90	0.38	93	0.12	93	0.04
Low-p_{T} (cut-based)	86	0.82	95	0.71	97	0.17	97	0.07
Low-p_{T} (multivariate)	88	0.73	96	0.66	97	0.17	97	0.07
High-p_{T}	45	0.34	79	0.60	80	0.13	80	0.05

Eur. Phys. J. C 81 (2021) 578

Muon working points in ATLAS Run 2

Medium

Within the ID acceptance $|\eta| < 2.5$, the *Medium* WP accepts only CB and IO muons. These are required to have at least two precision stations, except in the region $|\eta| < 0.1$, where muons with only one precision station are also included provided they have at most one precision hole station. The q/p compatibility is required to be less than seven to ensure a loose agreement between the ID and MS measurements. The acceptance is extended outside the ID coverage by including ME and SiF muons, required to have at least three precision stations, in the range $2.5 < |\eta| < 2.7$. Among prompt muons passing the *Medium* WP in $t\bar{t}$ events, more than 98% are CB muons.

Loose

The *Loose* selection WP accepts all the muons passing the *Medium* WP. In addition, it includes CT and ST muons in the range $|\eta| < 0.1$, where the gap in the MS coverage leads to a loss of efficiency for CB muon reconstruction. To increase the efficiency of the *Loose* criteria for low-p_T muons, IO muons with p_T below 7 GeV and only one precision station are accepted in the range $|\eta| < 1.3$, provided they are independently reconstructed also as ST muons. Requiring that IO muons are independently confirmed by the ST reconstruction strategy significantly increases their purity. Among prompt muons passing the *Loose* WP in $t\bar{t}$ events, about 97% are CB or IO muons. Approximately 1.5% are CT and ST muons in the region $|\eta| < 0.1$, among which the majority are CT muons. The efficiency increase of the *Loose* WP compared to *Medium* is around 20% for 3 GeV $< p_T <$ 5 GeV and approximately 1–2% for higher p_T.

Tight

Among the muons passing the *Medium* selection WP, only CB and IO muons with at least two precision stations are accepted for the *Tight* WP. The normalised χ^2 of the combined track fit is required to be less than 8 to reject pathological tracks due to hadron decays in flight. Further requirements are placed on the q/p compatibility and ρ' depending on the p_T and $|\eta|$ of the muon. These are optimised to provide better background rejection for lower-p_T muons, because of the higher expected non-prompt background at low p_T. In the optimisation, the rejection of non-prompt muons is maximised for a given target prompt-muon efficiency that rises from approximately 91% at p_T = 4 GeV to 95% at p_T = 9 GeV and approaches 96% as the p_T approaches 20 GeV. For the region 6 GeV $< p_T <$ 20 GeV, the *Tight* WP achieves a background reduction of more than 50% compared to *Medium*, with a corresponding efficiency loss for prompt muons of approximately 6%.

$$\rho' = \frac{|p_{T,ID} - p_{T,MS}|}{p_{T,CB}}$$

Eur. Phys. J. C 81 (2021) 578

Tag and Probe method

Eur. Phys. J. C 81 (2021) 578

- **Select sample containing di-muon pairs** (61 GeV $< m_{\mu\mu} <$ 121 GeV, opposite charge)

- **Tag muon**
  - Muon that fires trigger and passes stringent selections: high p_T, Medium quality and isolation

- **Probe muon**
  - Loosely reconstructed muons, no stringent requirements (p_T > 3 GeV)
  - Used to compute the efficiency for a certain selection

$$\epsilon\,(X|P) = \frac{N_P^X}{N_P^{\mathrm{All}}}$$

- The probe is used to test the efficiency of a certain reconstruction algorithm or of certain selection criteria

- Probes are usually required to be reconstructed with a detector subsystem independent of the one under study

- In simulation, to eliminate any background contamination, both the tag and the probe muons are required to be a prompt muon at generator level

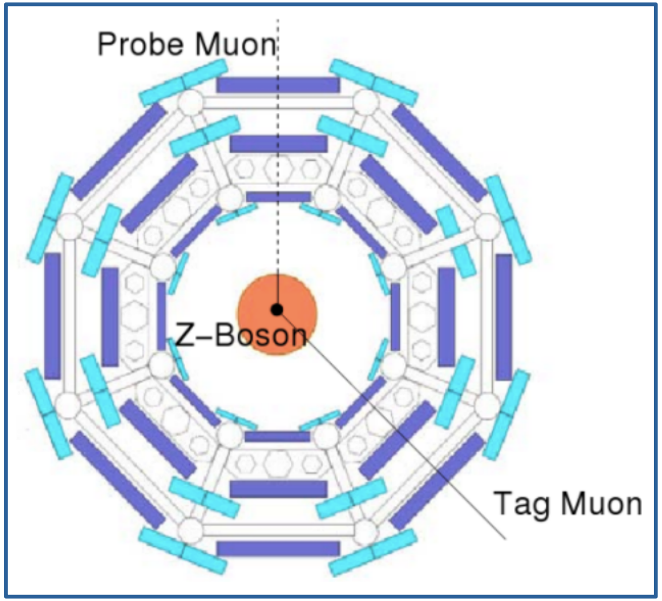

Muon reconstruction and identification efficiency

- **Left**: reconstruction and identification efficiency for muon tracks with $p_T > 10$ GeV in the Inner Tracker
- **Right**: reconstruction and identification efficiency for muons with $p_T > 10$ GeV satisfying the Medium quality criteria

$Z \rightarrow \mu\mu$

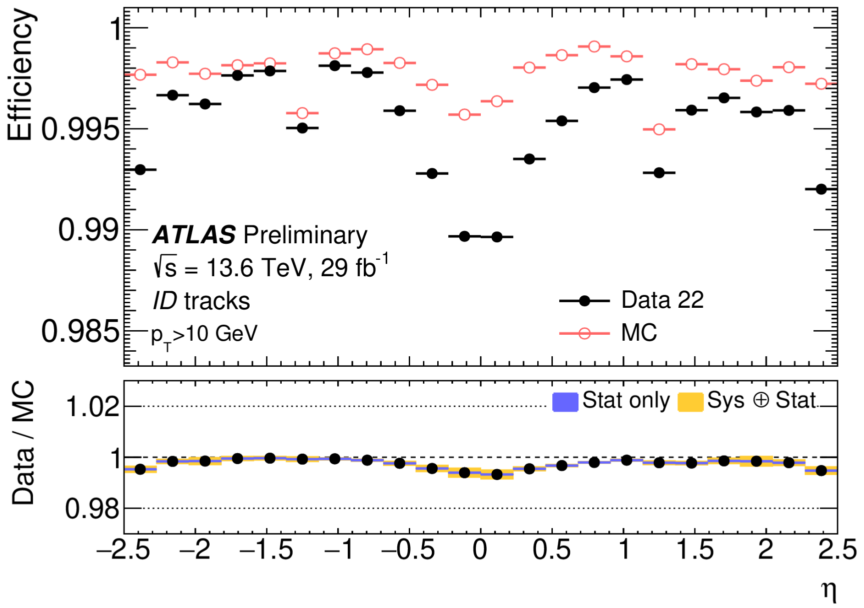

Acceptance hole at η~0 due to space for services

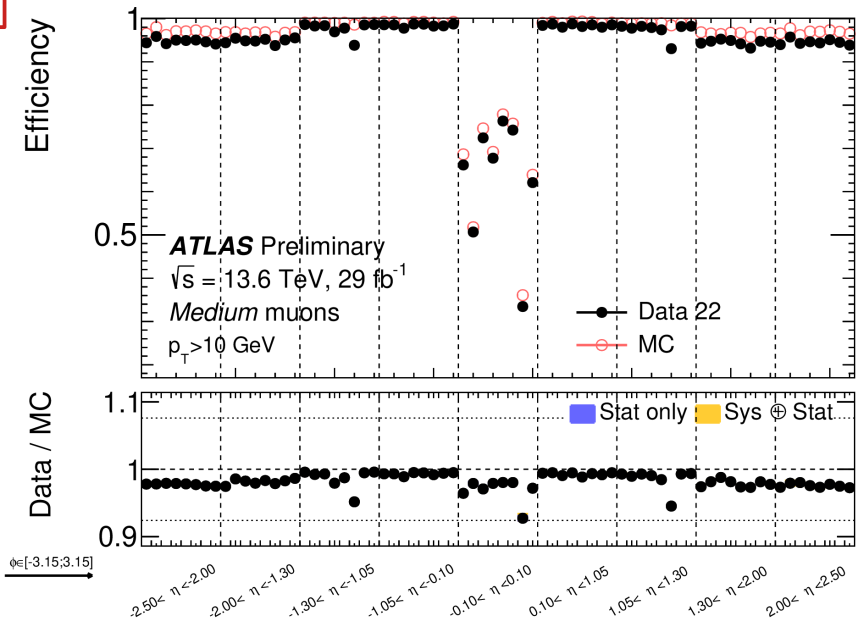

MUON-2023-01

Isolation Working Point

Eur. Phys. J. C 81 (2021) 578

Table 2: Definitions of the muon isolation WPs. The criteria used are listed in the second column, while the requirement on the minimum track p_{T} is shown in the third column. WPs marked with * exist in two variants: one with the cone ΔR parameter decreasing with p_{T}^{μ} as $\min(10\ \mathrm{GeV}/p_{\mathrm{T}}^{\mu}, 0.3)$, the other remaining constant at $\Delta R = 0.2$ for $p_{\mathrm{T}}^{\mu} > 50$ GeV.

Isolation WP	Definition	Track p_{T} requirement
*PflowLoose** *PflowTight**	$(p_{\mathrm{T}}^{\mathrm{varcone30}} + 0.4 \cdot E_{\mathrm{T}}^{\mathrm{neflow20}}) < 0.16 \cdot p_{\mathrm{T}}^{\mu}$ $(p_{\mathrm{T}}^{\mathrm{varcone30}} + 0.4 \cdot E_{\mathrm{T}}^{\mathrm{neflow20}}) < 0.045 \cdot p_{\mathrm{T}}^{\mu}$	$p_{\mathrm{T}} > 500$ MeV
*Loose** *Tight**	$p_{\mathrm{T}}^{\mathrm{varcone30}} < 0.15 \cdot p_{\mathrm{T}}^{\mu}$, $E_{\mathrm{T}}^{\mathrm{topocone20}} < 0.3 \cdot p_{\mathrm{T}}^{\mu}$ $p_{\mathrm{T}}^{\mathrm{varcone30}} < 0.04 \cdot p_{\mathrm{T}}^{\mu}$, $E_{\mathrm{T}}^{\mathrm{topocone20}} < 0.15 \cdot p_{\mathrm{T}}^{\mu}$	$p_{\mathrm{T}} > 1$ GeV
HighPtTrackOnly *TightTrackOnly**	$p_{\mathrm{T}}^{\mathrm{cone20}} < 1.25$ GeV $p_{\mathrm{T}}^{\mathrm{varcone30}} < 0.06 \cdot p_{\mathrm{T}}^{\mu}$	$p_{\mathrm{T}} > 1$ GeV
PLBDTLoose (PLBDTTight)	$p_{\mathrm{T}}^{\mathrm{varcone30}} < \max(1.8\ \mathrm{GeV}, 0.15 \cdot p_{\mathrm{T}}^{\mu})$ BDT cut to mimic *TightTrackOnly* (*Tight*) efficiency	$p_{\mathrm{T}} > 1$ GeV

Isolation Working Point

Eur. Phys. J. C 81 (2021) 578

	$3 < p_T$ [GeV] < 5		$5 < p_T$ [GeV] < 20		$20 < p_T$ [GeV] < 100		$p_T > 100$ GeV	
Isolation WP	ϵ_μ [%]	ϵ_{HF} [%]	ϵ_μ [%]	ϵ_{HF} [%]	ϵ_μ [%]	ϵ_{HF} [%]	ϵ_μ [%]	ϵ_{HF} [%]
Loose	63	14.3	86	7.2	97	6.1	99	12.7
Tight	53	11.9	70	4.2	89	1.0	98	1.6
PflowLoose	62	12.9	86	6.8	97	5.0	99	9.1
PflowTight	45	8.5	63	3.1	87	0.9	97	0.8
HighPtTrackOnly	92	35.9	92	17.2	92	4.5	92	0.6
TightTrackOnly	80	19.9	81	7.0	94	3.2	99	3.3
PLBDTLoose	81	17.4	83	5.1	93	1.3	98	1.7
PLBDTTight	57	9.6	69	2.7	87	0.5	98	1.7

Isolation Working Point

Eur. Phys. J. C 81 (2021) 578

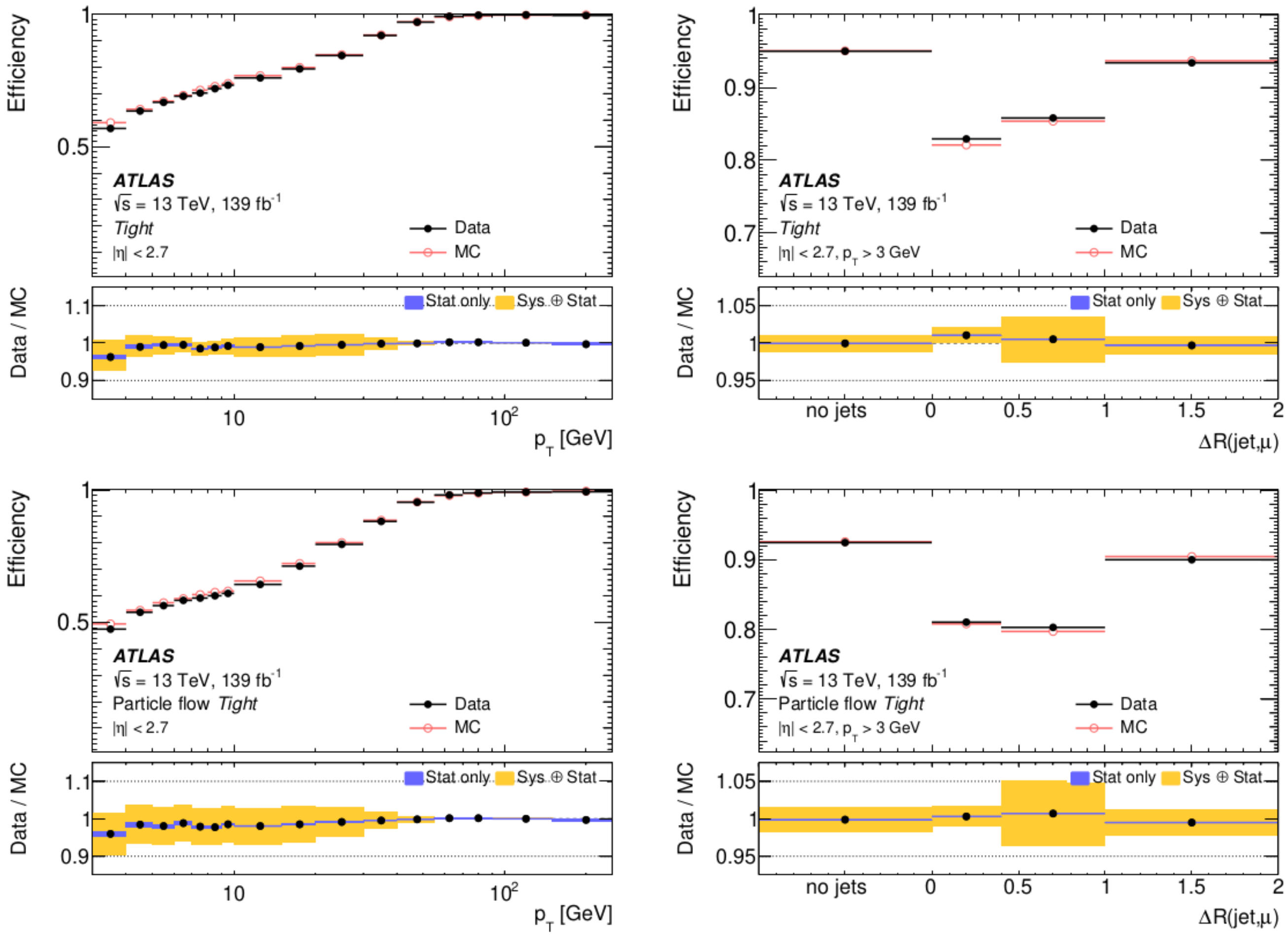

Muon reconstruction and identification efficiency vs pile-up

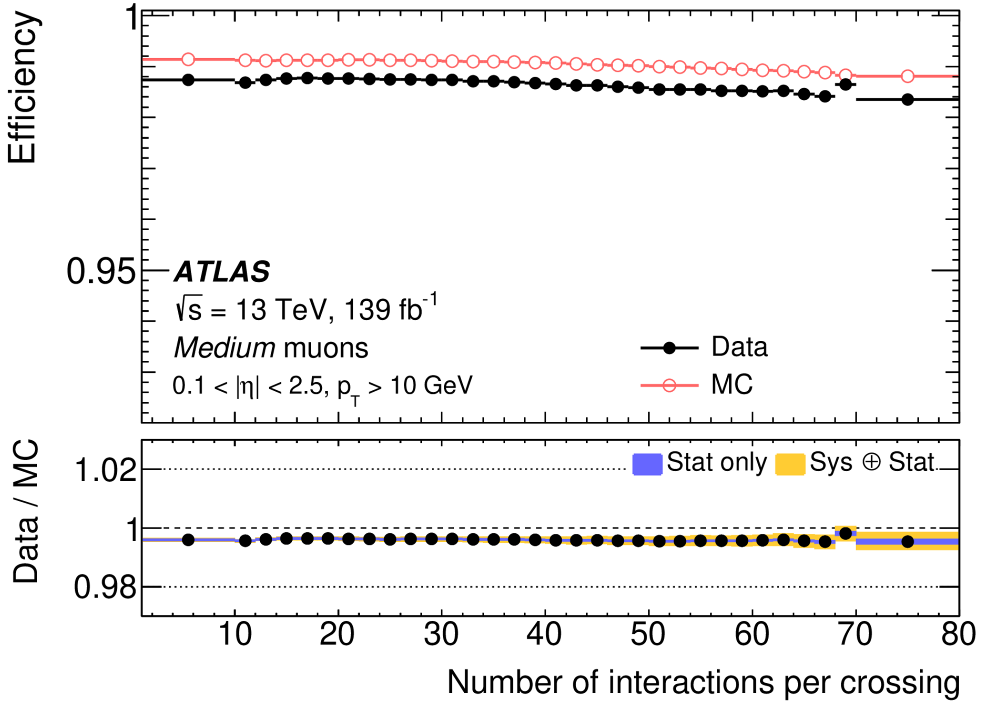

Eur. Phys. J. C 81 (2021) 578

Main systematic uncertainties

- The main uncertainty on the **muon momentum scale** arises from performing the calibration using only Z or J/Psi decays, instead of combining both

- The main uncertainty on the **muon momentum resolution** arises from varying the p_T ranges used in the fit

- The main uncertainty on the **muon reconstruction and identification efficiency** arises from possible biases
  in the tag-and-probe method, such as biases due to different kinematic distributions between reconstructed probes and generated muons or correlations between ID and MS efficiencies (so called "T&P method" uncertainty)

- Other sources of uncertainty include the choice of $m_{\mu\mu}$ range and binning and the parametrization of the J/Psi background

Systematic uncertainties on efficiency SFs (Run 2)

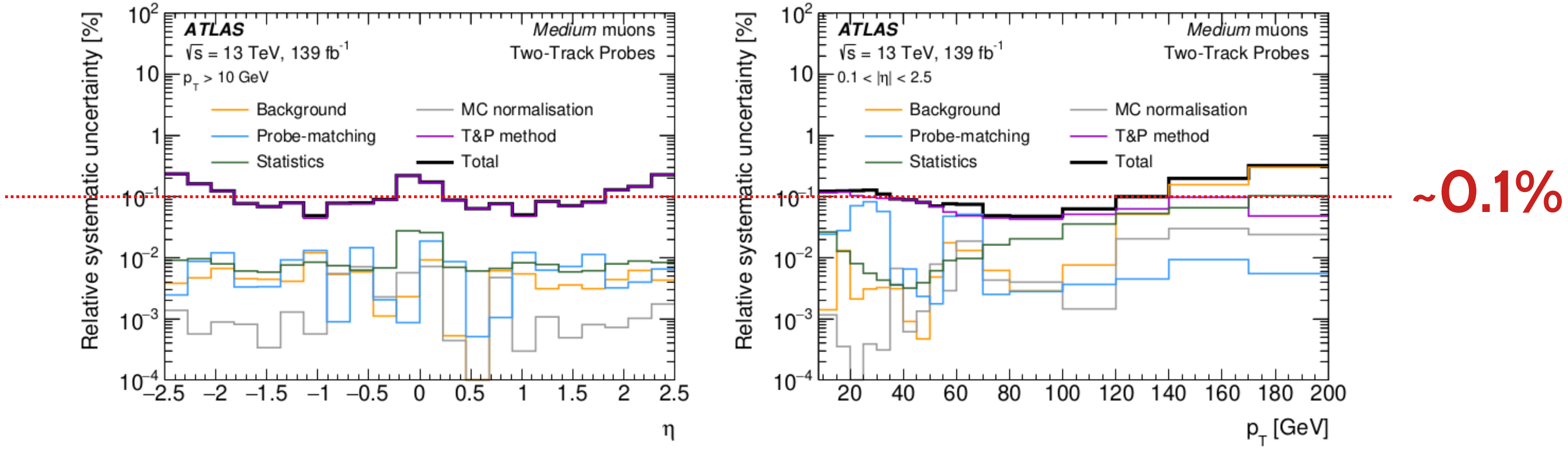

Figure 7: Relative contributions to the systematic uncertainty in the efficiency SFs for *Medium* muons measured with $Z \to \mu\mu$ decays, as a function of η (left) and p_{T} (right) for muons with $p_{\mathrm{T}} > 10$ GeV, and integrated over the other kinematic observables. The uncertainty depicted as *Background* is the sum in quadrature of the *Template shape*, Λ-*SC*, and *Background fit* uncertainties, whereas the *MC normalisation* comprises the *Cross-section* and *Luminosity* uncertainties. The total uncertainty is the sum in quadrature of the individual contributions.

The $Z \to \mu\mu$ sample allows the reconstruction and identification efficiencies to be measured with a precision better than the per-mille level for muons with p_{T} above 10 GeV in most of the detector regions. The $J/\psi \to \mu\mu$ sample extends the measurement down to $p_{\mathrm{T}} = 3$ GeV, with a precision better than 1% in the 5–20 GeV range.

Eur. Phys. J. C 81 (2021) 578

Sagitta bias

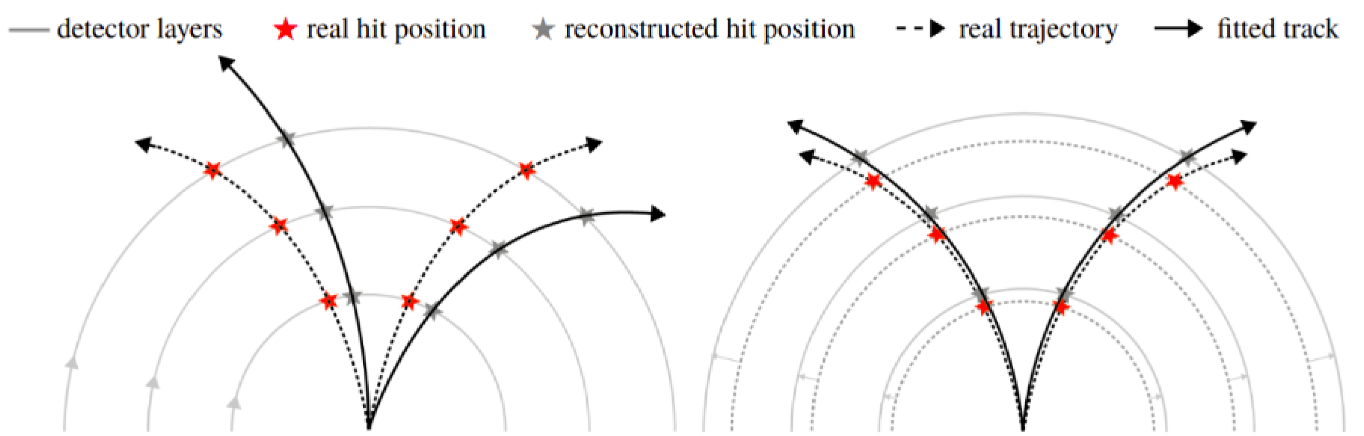

Figure 4: Visualisation of a possible sagitta bias (left) due to a rotation of detector layers and length-scale bias (right) due to a radial expansion of detector layers. (Image: ATLAS Collaboration/CERN)

Opposite effects on positively and negatively charged particles

Affecting positive and negative particles equally

New Small Wheel: detector technologies

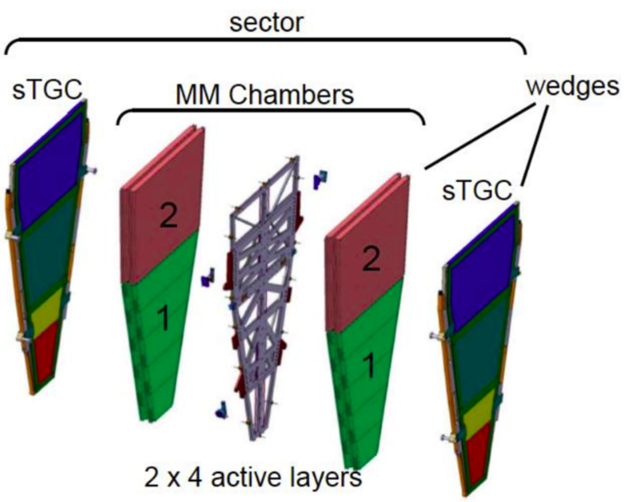

Each wedge is a quadruplet of detector layers

Micromegas

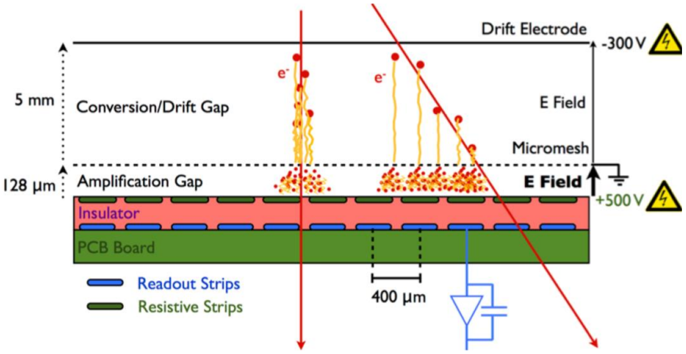

sTGC

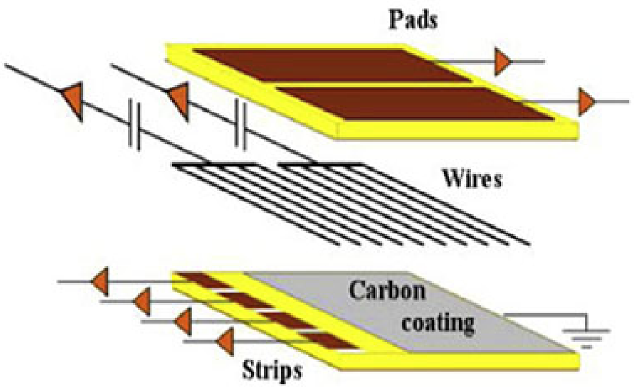

Micromegas detectors

- High-precision detectors that can handle higher rates than MDTs
- 8 layers per sector per side
- Expect <100 µm precision per plane

sTGC detectors

- Provide trigger in the end-cap region
- 8 layers per sector per side
- Similar to old TGCs, but smaller strips to handle higher rates
- 1 mrad resolution for the reconstructed segment angle in the trigger

New Small Wheel: Micromegas

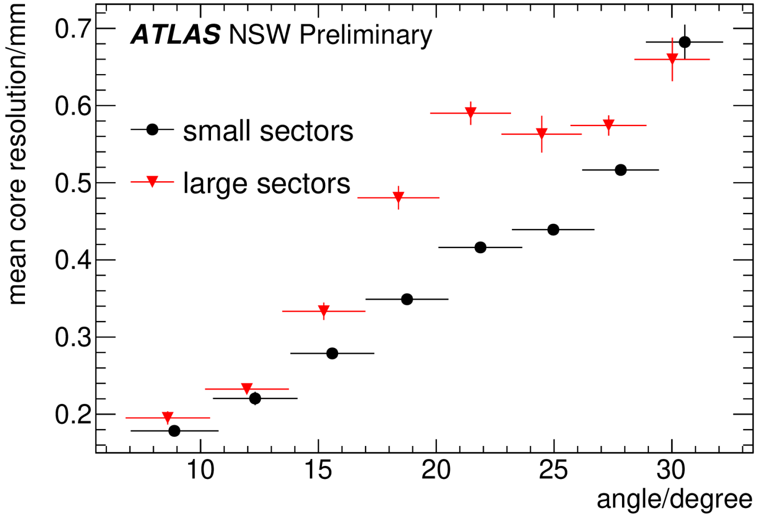

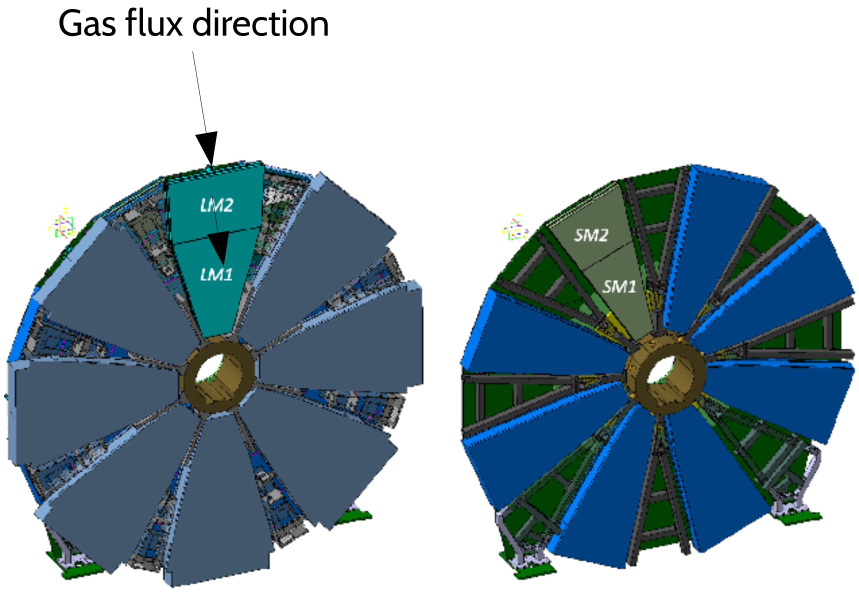

Physics cases

$$H \rightarrow \mu\mu$$

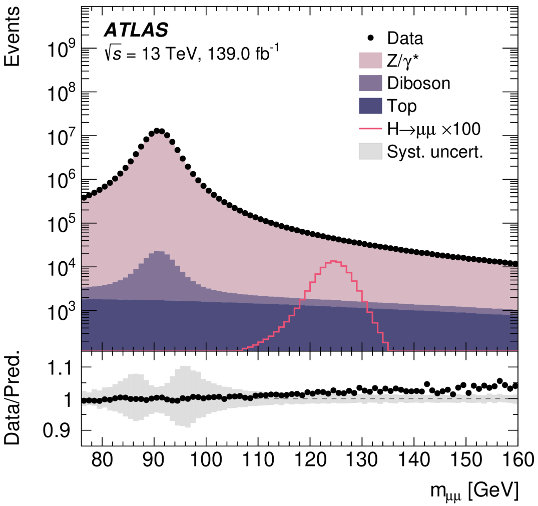

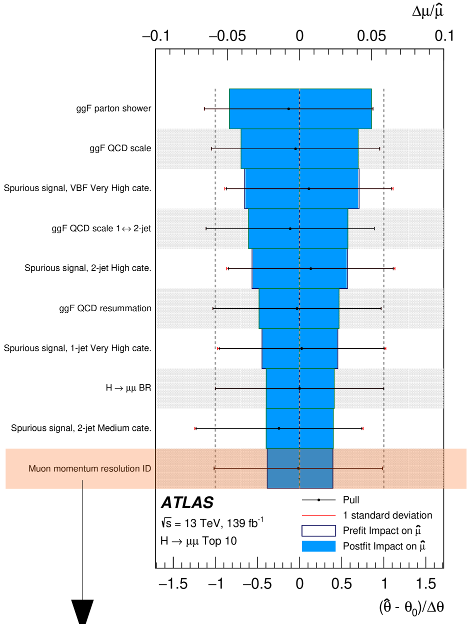

Muon momentum resolution

Phys. Lett. B 812 (2021) 135980

Signal strength = 1.2 ± 0.6
Observed (expected) significance in only bkg hypothesis 2.0σ (1.7σ)

$H \rightarrow ZZ^* \rightarrow 4l$
$\sqrt{s}$ = 13 TeV, 139 fb^{-1}

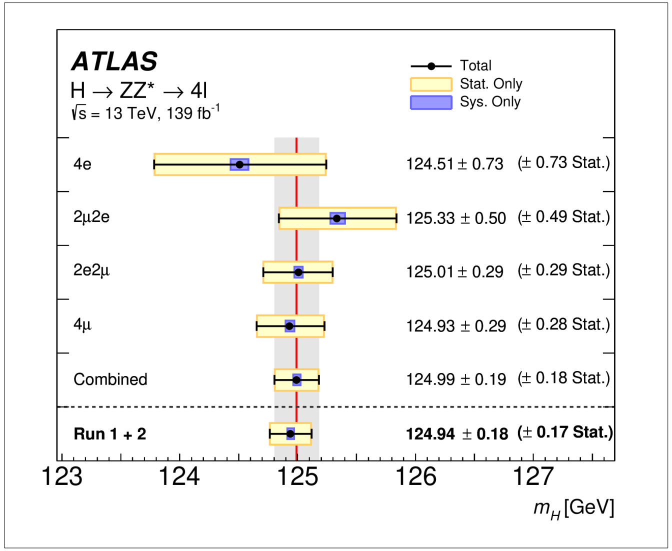

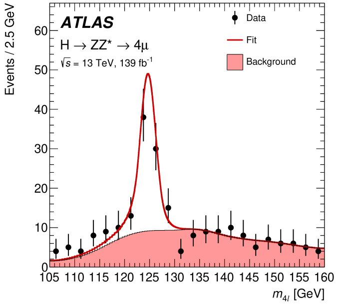

arXiv:2207.00320

$$m_H = 124.99 \pm 0.18(\text{stat.}) \pm 0.04(\text{syst.})\ \text{GeV}$$

Systematic Uncertainty	Contribution [MeV]
Muon momentum scale	±28
Electron energy scale	±19
Signal-process theory	±14